Journal of Radiation Research, 2015, 56, 248–260
doi: 10.1093/jrr/rru095 Advance Access Publication 3 November 2014

Whole-thorax irradiation induces hypoxic respiratory failure, pleural effusions and cardiac remodeling

Meetha MEDHORA[1,2,3,4,*], Feng GAO[1], Chad GLISCH[1], Jayashree NARAYANAN[1], Ashish SHARMA[1], Leanne M. HARMANN[2,5], Michael W. LAWLOR[6], Laura A. SNYDER[7], Brian L. FISH[1], Julian D. DOWN[8], John E. MOULDER[1], Jennifer L. STRANDE[2,5] and Elizabeth R. JACOBS[2,3,4]

[1]Department of Radiation Oncology, Medical College of Wisconsin, 8701, Watertown Plank Road, Milwaukee, WI 53226, USA
[2]Cardiovascular Center, Medical College of Wisconsin, 8701, Watertown Plank Road, Milwaukee, WI 53226, USA
[3]Division of Pulmonary Medicine, Medical College of Wisconsin, 8701, Watertown Plank Road, Milwaukee, WI 53226, USA
[4]Research Service, Department of Veteran's Affairs, Clement J. Zablocki VA Medical Center, Milwaukee, Wisconsin, USA
[5]Division of Cardiovascular Medicine, Medical College of Wisconsin, 8701, Watertown Plank Road, Milwaukee, WI 53226, USA
[6]Division of Pediatric Pathology, Medical College of Wisconsin, 8701, Watertown Plank Road, Milwaukee, WI 53226, USA
[7]Marshfield Laboratories; Wisconsin Veterinary Referral Hospital, Waukesha, Wisconsin, USA
[8]Harvard–Massachusetts Institute of Technology Division of Health Sciences Technology, Massachusetts Institute of Technology, Cambridge, Massachusetts, USA
*Corresponding author. MFRC 4076, Medical College of Wisconsin, 8701, Watertown Plank Road, Milwaukee, WI 53226, USA. Tel: +1-414-955-5612; Fax: +1-414-955-6459; Email: medhoram@mcw.edu

(Received 7 July 2014; revised 11 September 2014; accepted 19 September 2014)

To study the mechanisms of death following a single lethal dose of thoracic radiation, WAG/RijCmcr (Wistar) rats were treated with 15 Gy to the whole thorax and followed until they were morbid or sacrificed for invasive assays at 6 weeks. Lung function was assessed by breathing rate and arterial oxygen saturation. Lung structure was evaluated histologically. Cardiac structure and function were examined by echocardiography. The frequency and characteristics of pleural effusions were determined. Morbidity from 15 Gy radiation occurred in all rats 5 to 8 weeks after exposure, coincident with histological pneumonitis. Increases in breathing frequencies peaked at 6 weeks, when profound arterial hypoxia was also recorded. Echocardiography analysis at 6 weeks showed pulmonary hypertension and severe right ventricular enlargement with impaired left ventricular function and cardiac output. Histologic sections of the heart revealed only rare foci of lymphocytic infiltration. Total lung weight more than doubled. Pleural effusions were present in the majority of the irradiated rats and contained elevated protein, but low lactate dehydrogenase, when compared with serum from the same animal. Pleural effusions had a higher percentage of macrophages and large monocytes than neutrophils and contained mast cells that are rarely present in other pathological states. Lethal irradiation to rat lungs leads to hypoxia with infiltration of immune cells, edema and pleural effusion. These changes may contribute to pulmonary vascular and parenchymal injury that result in secondary changes in heart structure and function. We report that conditions resembling congestive heart failure contribute to death during radiation pneumonitis, which indicates new targets for therapy.

Keywords: radiation pneumonitis; mast cells; right ventricular mass; tachypnea

INTRODUCTION

The lung exhibits a steep dose-related response to ionizing radiation [1, 2] such that there is no lethality with 12 Gy to the thorax by 60 days but there are no survivors following pneumonitis with 15 Gy in WAG/RijCmcr (Wistar) rats. Radiation typically induces two phases of injury: pneumonitis occurring after a few weeks, and chronic fibrosis that develops months to years later [1, 3]. In spite of decades of research the pathophysiological mechanisms for lethal radiation-induced lung injury at the organ level remain uncertain. Epithelial cells in the lung [3, 4] and vascular endothelial cells [3] are injured by radiation, while inflammatory infiltrates [4, 5] and edema [3] appear as secondary effects in the setting of high-single or fractionated radiation doses.

More recently, pulmonary vascular remodeling [6] and interaction between the heart and lungs [7] have been suggested as augmenting morbidity (concurrent with pneumonitis) 8 weeks after radiation to the whole or partial thorax of Wistar rats. In these studies, rats were irradiated with a single-fraction proton beam at doses of 15–20 Gy. In another study, increments in breathing rate (a non-invasive indicator of lung dysfunction) have been reported after radiation to the heart alone. This occurred 10 weeks after a single X-ray dose of 20 Gy, and 30 weeks after 15–17.5 Gy [8]. Using a single lower dose (10 Gy) to the whole thorax, transient right ventricular hypertrophy (RVH) was concurrent with the increase in breathing rate measured during the peak of pneumonitis [9, 10]. In the same model, increased pulmonary vascular resistance, reduced arteriolar density and decreased passive vascular distensibility that accompanied radiation pneumonitis were described *ex vivo* [9, 10]. Taken together, these findings implicate abnormalities to the vasculature of the lungs during radiation pneumonitis that then lead to right ventricular remodeling and pulmonary hypertension.

Radiation pneumonitis is associated with inflammatory infiltrates in the lungs [5] and may arise with or without pleural effusions [11]. While pneumonitis presents as a major and life-threatening complication, comprehensive assessments of the presence or absence of pleural effusions following whole lung exposure in upper-half body and total body irradiation in humans were not always reported [12–15]. From 5 to 20% of patients receiving high-dose localized radiotherapy exhibited non-malignant pleural effusions during radiation pneumonitis, a finding attributed by the authors to a pleural reaction [1, 16, 17]. Effusions at later times may occur in irradiated patients as a result of thoracic lymph vessel occlusion by mediastinal fibrosis [18]. In mice, the timing and volume of pleural effusions after radiation, as well as sensitivity to lung injury, varies between genetic strains [19]. The C57L strain is highly sensitive to lethal pneumonitis but does not develop effusions. C57BL/6 mice, on the other hand, present with late effusions (0.1–1.8 ml/mouse) together with a variable degree of pneumonitis [19]. In CBA mice, the pleural effusions follow the recovery from pneumonitis, whereas other strains, including the BALB/c strain, show earlier effusions that overlap with pneumonitis [19]. An early incidence of pleural effusions or hydrothorax has similarly been reported in whole-thorax irradiated WAG/RijCmcr rats and other rat strains [20, 21]. In the current study we used echocardiography to support evidence that lethal doses of radiation to the whole thorax of Wistar rats cause pulmonary hypertension and severe right ventricle (RV) enlargement. Hypoxia and cardiac dysfunction with edema/pleural effusions were associated with morbidity. We report that conditions that resemble congestive heart failure contribute to death during radiation pneumonitis, observations which position us well to investigate targeted mitigation in future studies.

Materials and Methods

Animal care

All animal protocols were approved by the Institutional Animal Care and Use Committee (IACUC). Based upon direction from the IACUC, rats were designated as morbid and euthanized if they met specified veterinarian's criteria. Rats were considered morbid if they showed 20% loss in body weight or met at least three of the following specified criteria: (i) greater than or equal to 10% loss in body weight; (ii) inactivity for one day, defined as no movement unless actively stimulated; (iii) lack of grooming that became worse after 24 h; (iv) breathing rates of less than 50 or greater than 250 breaths per minute or demonstration of open-mouth breathing or increased effort for breathing; (v) hunched posture on two consecutive days.

Animals and irradiation

The studies were done in unanesthetized female WAG/RijCmcr rats. The WAG/RijCmcr strain [22] (previously called WAG/RijMcw, WAG/RijY and WAG/Rij) has been used for normal tissue radiobiology studies at the Medical College of Wisconsin (MCW) [23, 24], Yale [25, 26] and in the Netherlands [21, 27–29] for decades. The radiation toxicity endpoints for bone marrow [30], skin [31], spinal cord [29], lung [27, 32], kidney [24, 33] and heart [33, 34], have been established in this strain. The strain is neither particularly radiosensitive nor radioresistant, and the lethal dose for whole-thorax irradiation is typical of the other rat strains that have been studied (for a review, see Hopewell *et al.* [35]).

The rats were irradiated at 9–10 weeks of age, which corresponded to a weight of 120–140 g [2]. The rats were placed in a Plexiglas jig and given 15 Gy of radiation to the thorax. An XRAD 320 orthovoltage system (Precision X-Ray, CT, USA) was used, with a 320-kVp beam, a half-value layer of 1.4 mm Cu, and a midline dose rate of 1.43 Gy/min. The absolute dose was measured with a calibrated Farmer-type ionization chamber. The radiation dose was delivered by two equally weighted parallel-opposed lateral beams to improve

the dose uniformity. A 30 mm (right–left) × 45 mm (up–down) collimator was used to define a radiation field that encompassed the whole thorax. The head, kidneys and GI tract were out of the field, while the heart and a small portion of liver were exposed.

In batches of 10–20, rats were irradiated as above and housed with age-matched unirradiated sibling controls. One group of rats was sacrificed after 6 weeks for invasive endpoints. This time-point was selected for study of the irradiated rats because, based on our studies with this model [2, 5, 9], all irradiated rats had developed pneumonitis. Given the steep radiation dose–response curve, we expected no survivors by 8 weeks [2]. A second group was followed for non-invasive endpoints until rats became morbid from radiation pneumonitis between 5 and 8 weeks after 15 Gy. Breathing rates (non-invasive) were taken 4, 6 and 8 weeks and pulse-oximetry (non-invasive) was conducted 5 and 6 weeks after irradiation in this group. Invasive assays such as lung histology, lung weights and heart weights in dissected hearts after echocardiography were conducted at 6 weeks after 15 Gy. Pleural effusions were also collected from these rats or those that reached the IACUC criteria for morbidity at 6 weeks after 15 Gy.

Breathing rate measurements

Breathing rates for each rat were measured every two weeks starting 4 weeks after exposure, as described previously [10, 36]. Rats were restrained in a Plexiglas jig, which was placed in a transparent, airtight box. A differential pressure transducer was connected to a data acquisition device (Dataq-DI 158U, Dataq Instruments Inc., Akron, OH, USA) to sense changes in pressure in the box. The frequency of pressure changes was recorded and analyzed. Recordings for a maximum of 10 min per animal after two training sessions were used. The mean breathing rate for each rat was then calculated from a minimum of four steady regions of the recording lasting greater than 15 s each.

Pulse oximetry

Oxygen saturation was measured in non-anesthetized rats using a veterinary pulse oximeter (Nonin, 8600V series, Plymouth, MN, USA) [37] connected to a computer with WinDaq data acquisition and analysis software [10]. Rats were acclimated to a jig placed on a warming plate (40°C) 2–3 days prior to measurements. On the day the measurements were made, a probe was positioned over the tail artery in restrained rats, and recordings from the oximeter were captured over 5–10 min. Steady traces with stable pulse readings in the physiological range were analyzed. The mean value for each rat was computed by an operator blinded to the treatment of the rat. Average measurements were obtained from three separate segments of recording 10–20 s in duration.

Wet/dry weight

After the rats were euthanized, the lower lobe of the right lung was harvested, gently wiped and immediately weighed. The same sample was dried at 60–80°C for 24 h. After drying, the lung piece was weighed again to calculate the ratio of wet to dry weight.

Histology of lung

Rats were anesthetized with isoflurane. After removal of the heart and lungs from the chest, lungs were fixed, inflated with 10% neutral buffered formalin (Fisher Scientific, Pittsburg, PA) introduced through the airways, and then embedded in paraffin [5, 10, 36]. Whole mount sections of the left lung were cut (4 μm), processed and stained with hematoxylin & eosin (H&E) (Richard Allan, Kalamazoo, MI). All histological work was performed at the Pediatric Biobank and Analytic Tissue Core. Histological scores were obtained from four endpoints in H&E-stained lung sections: (i) vascular wall thickness; (ii) foamy macrophages; (iii) alveolar wall thickness; and (iv) erythrocyte score (a measure of perfusion). Histologic morphometrics were performed on five randomly selected fields per slide; this was done independently in a blinded manner by the three observers (for a total of 15 sections). The scoring system was constructed so that higher scores reflected more severe pathology. Foamy macrophages and vascular wall thickness were analyzed as described [20]. Alveolar wall thickness was scored on a five-point scale from five fields per rat (randomly selected over a whole mount section of the lung): 0 = all alveoli were inflated with lacy appearance; 1 = mild to moderate thickening in some alveoli; 2 = thickening with signs of consolidation; 3 = thickening with >25% consolidated areas; 4 = thickening with >50% consolidated areas. For scoring erythrocytes, thresholds were chosen for red-colored pixels with a hue that was specific to erythrocytes, and that did not select eosin-stained or other material. Identical parameters for hue, saturation, brightness and background values were used for all samples. The number of pixels obtained were divided into four equal bins and scored as follows: 1 = highest values in top 75% bin; 2 = 50–75%; 3 = 25–49%; 4 ≤ 25%. Scores from all categories were summated for a total histology score shown in Table 1.

Echocardiography

Transthoracic echocardiography was performed in anesthetized (2% isoflurane) animals at 6 weeks after radiation or at the corresponding time in unirradiated, age-matched controls. Measurements and data analyses were performed by an investigator blinded to the study groups. Animals were studied in the left lateral decubitus position with a commercially available echocardiographic system (Vivid 7, General Electric, with an 11-MHz M12-L linear array transducer, GE Healthcare, Waukesha, WI). Transthoracic echocardiography

Table 1. Summary of lung-related structure and function 42 days after 15 Gy

Parameters at 42 days	0 Gy		15 Gy		$P < 0.05$ 0 Gy vs 15 Gy
	Mean ± SD	*n*	Mean ± SD	*n*	
Body weight (gram)	167 ± 7	13	140 ± 11	30	yes
Breathing rate (breaths/minute)	135 ± 13	4	269 ± 44	8	yes
Arterial oxygen saturation (%)	92 ± 3	4	75 ± 13	8	yes
Whole lung wet weight (gram)	0.7 ± 0.1	9	1.5 ± 0.3	23	yes
Lung wet:dry weight	4.4 ± 0.1	8	4.6 ± 0.2	15	yes
Pleural effusions (milliliter)	0 ± 0	15	2.5 ± 2.5	33	yes
Histology score (sum of 4 categories)	2.8 (2.1–4.4) Median (25–75%)	4	7.8 (6.0–9.1) Median (25–75%)	8	yes
Right ventricular hypertrophy (RV/LV + S)	0.23 ± 0.06	4	0.44 ± 0.08	8	yes

SD = standard deviation, R = right, L = left, V = ventricle, S = septum.

was performed from the cardiac short axis of the left ventricle at the papillary muscle level, using the anatomical M-mode feature of the Vivid 7 echo. An M-mode display was generated from raw data 2D images with the line selected passing through the anterior and inferior segments. Stroke volume (SV) was measured using left ventricular end diastolic volume (EDV) and end systolic volume (ESV) using the formula SV = EDV − ESV. Ejection fraction (EF) was measured using the formula EF = SV/EDV*100 [38]. Cardiac output was calculated by multiplying the heart rate × SV. The LV mass was derived from the anteroseptal thickness (AST) and inferolateral thickness (ILT) using the formula: 0.8 (1.04[(ILT + LVIDd + AST)^3 − LVIDd3]) + 0.6 [38]. Three consecutive heart beats were measured and the average used for analysis.

Right ventricular weight

The heart was harvested and the right ventricle was dissected [9]. Right ventricular hypertrophy was assessed as the ratio of the weight of the right ventricle to the weight of the left ventricle plus septum (RV/LV + S) [9].

Histology of heart

In dedicated experiments, irradiated rats ($n = 10$) that received 15 Gy to the thorax and unirradiated controls ($n = 6$) were anesthetized with isoflurane at 8 weeks after irradiation. The hearts were perfused with 10 ml of cardioplegic solution (1M KCl and 5 g/dl dextrose (D-glucose)) for 10 min. Each heart was removed, cleaned of adjoining tissues such as the pulmonary artery and aorta and dried on a paper towel. The atria were removed and the apex was cut, leaving 3–4 mm of the ventricles. The right ventricle free wall was dissected out from the left ventricle at the A–V line and marked with ink at the base to orient the samples for embedding in paraffin. The left ventricle was cut with the septum and was similarly marked at the base with ink. The tissues were fixed in 10% neutral buffered formalin for 24–48 h prior to embedding in paraffin. Samples were sectioned at 4 μm and stained with hematoxylin and eosin (H&E). The sections were then examined in a blinded manner by a pathologist and a cardiologist. All abnormalities observed were scored. The samples were decoded after analysis.

Collection of pleural fluid

For collections of pleural fluid, animals were anesthetized with isoflurane; an anterior thoracotomy was performed and all visible fluid in the pleural cavity collected. Blood was collected from the heart by cardiac puncture. Effusions and blood were assessed by a Clinical Laboratory Improvement Amendments (CLIA)-approved veterinary laboratory (Marshfield Laboratories). The inflammatory cell populations were determined by light microscopic analysis of Romanowsky-stained cytospin preparations of the fluid. A 100-cell differential count was performed for each effusion to determine the relative percentages of cells.

Protein assay

Total protein in the pleural fluid or serum was estimated by the Coomassie Brilliant Blue method using a Bio-Rad Protein Assay Kit (Cat. #500-0002, Bio-Rad, Hercules, CA, USA). The fluids were centrifuged at 10 000*g* before the assay to remove cellular debris.

Statistical analysis

All data are shown as means with standard deviations and number of animals, except for histology scores, which are medians with 25–75% ranges. For the multi-group comparisons in Figs 1–3, the significance of differences was assessed

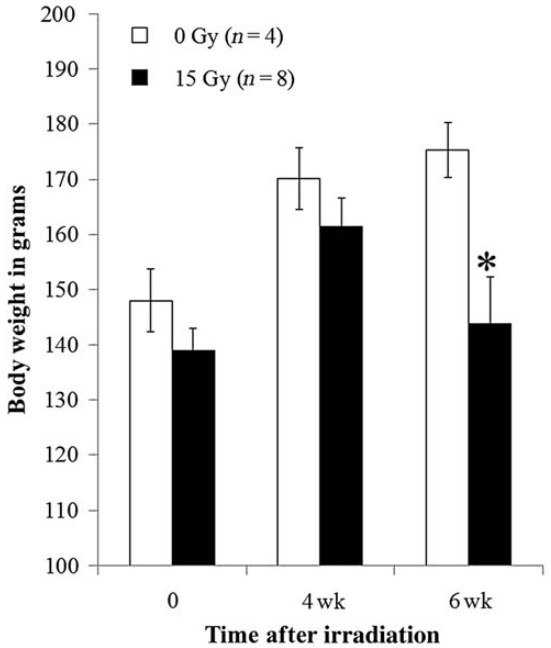

Fig. 1. Radiation-induced decrease in body weight. Graph shows body weights (mean with standard deviation) of rats in grams at time of irradiation and 4 and 6 weeks after irradiation. Irradiated rats (15 Gy) had lower body weight than unirradiated control rats at 6 weeks ($*P < 0.05$). No difference was observed for results between the irradiation group and control at the other time-points. n = number of rats.

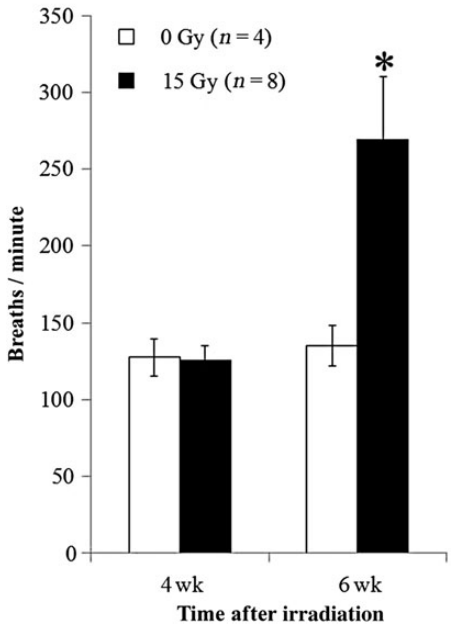

Fig. 2. Radiation-induced increase in breathing rate. Breaths per minute (Y-axis) are presented as means with standard deviations. Irradiated rats (15 Gy) had higher breathing rate than unirradiated (control) rats at 6 weeks ($*P < 0.05$). No difference was observed for results between the irradiated group and controls at 4 weeks. n = number of rats.

with ANOVA with the Holm-Sidak methods for dealing the multiple comparison issues. For the two-group comparisons in Tables 1 and 2 the significances of differences were determined by *t*-tests or by Mann–Whitney (the latter for histology scores).

Results

Overall health and lung-related injury after 15 Gy

Body weights in irradiated and control rats were obtained immediately prior to irradiation, and at 4 and 6 weeks after irradiation, as an index of overall health (Fig. 1 and Table 1). By 6 weeks after irradiation, the weight of treated rats was below that of their control littermates (Fig. 1 and Table 1). Breathing rates appear in Fig. 2 and Table 1. Irradiated and control rats have similar breathing rates at 4 weeks, but by 6 weeks following 15 Gy irradiated rats developed tachypnea. Irradiated rats had lower values of arterial oxygen saturation than that of controls and that of the same rats examined at 5 weeks (Fig. 3 and Table 1). Lungs from irradiated rats doubled in wet weight and were visibly larger in size than those of control animals (Table 1). There was a modest increase in the wet:dry weight ratio of the lungs, which could be due to a protein-rich edema as well as an increase in cellularity (Table 1). Lung histology showed increased

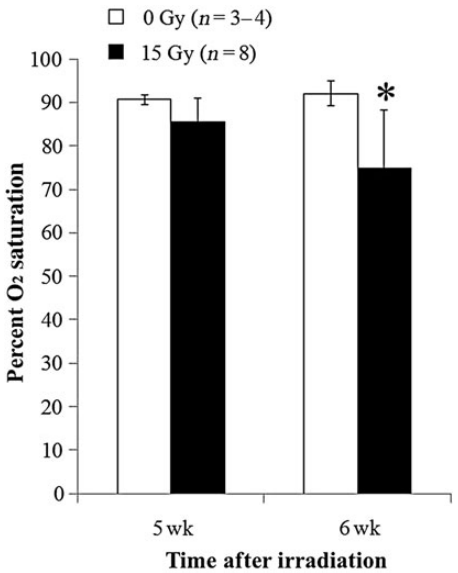

Fig. 3. Radiation-induced hypoxia. Percent oxygen (O_2 saturation, y-axis) is presented as means with standard deviations. Rats had lower percent O_2 saturation at 6 weeks after 15 Gy irradiation than unirradiated controls ($*P < 0.05$ between irradiated and unirradiated, and between irradiated at 5 vs 6 weeks). No difference was observed for results between the irradiated group and controls at 5 weeks. n = number of rats.

Table 2. Summary of cardiac structure and function at 42 days after 15 Gy

Echocardiogram at 42 days	Abbreviation definition	Mean ± SD (n = 5–6 rats/group)		$P < 0.05$ 0 Gy vs15 Gy
		0 Gy	15 Gy	
RV width (cm)	right ventricular width	0.23 ± 0.06	0.44 ± 0.06	yes
RV free wall (cm)	right ventricular free wall	0.09 ± 0.02	0.14 ± 0.05	yes
LVIDd (cm)	left ventricular internal dimension (diastole)	0.60 ± 0.05	0.44 ± 0.11	yes
EDV (T) (ml)	end-diastolic volume	0.51 ± 0.11	0.23 ± 0.14	yes
SV (ml)	stroke volume	0.44 ± 0.12	0.17 ± 0.09	yes
HR (beats/min)	heart rate	421 ± 37	307 ± 46	yes
CO (ml/min)	cardiac output	187 ± 55	55 ± 31	yes
TR	tricuspid regurgitation (leaking tricuspid valve)	unmeasurable	moderate	
Max velocity (m/s)	maximum velocity	unmeasurable	3.03 ± 0.39	
Pressure gradient (mm Hg)	pressure gradient	unmeasurable	38.0 ± 10.1	
TPVR ($ms^{-1}m$)	total pulmonary vascular resistance	unmeasurable	214 ± 35	
MPA end-diastolic pressure (mm Hg)	main pulmonary artery end-diastolic pressure	unmeasurable	6.8 ± 1.7	
RVOT VTI (cm)	right ventricular outflow tract	unmeasurable	1.5 ± 0.4	
PASP (mm Hg)	pulmonary artery systolic pressure	unmeasurable	74 ± 8	
PAT (ms)	pulmonary acceleration time	30.7 ± 8.6	13.0 ± 2.1	yes
PAT/ET	Indicator for pulmonary hypertension	42.2 ± 6.6	19.0 ± 4.2	yes
IVRT (ms)	isovolumetric relaxation time	14.6 ± 2.5	39.6 ± 7.6	yes
e' (m/s)	early diastolic mitral annulus velocity	0.08 ± 0.2	0.03 ± 0.1	yes

inflammatory cells as well as alveolar and vessel wall thickness, but a decrease in erythrocytes in irradiated lungs (Fig. 4). Summated histological scores for these parameters (see Methods and Table 1) were higher in irradiated rats than controls. The presence and volume of pleural effusions was variable (0–8.5 ml), occurring in 76% of irradiated rats but not in unirradiated controls (Table 1). An increase in the right ventricular mass was observed after 15 Gy (Table 1).

Cardiac structure and function after 15 Gy (see Table 2 and Fig. 5)

The 2D imaging of the heart in irradiated rats showed severe right ventricular enlargement with the interventricular septum compressing the left ventricle and reducing the diastolic or filling volume. The heart rate and stroke volume were also reduced, consistent with compromised left ventricular refilling, and cardiac outputs in irradiated rats were decreased to ~30% that of control rats. Doppler-derived parameters showed that tricuspid regurgitation occurred only in irradiated rats with markedly reduced pulmonary acceleration time, while the ventricular relaxation times were more than doubled. Pulmonary artery profiles reflected the development of severe pulmonary hypertension.

No histological abnormalities were observed in H&E-stained sections of the heart from 4/10 irradiated rats or from any of the 6/6 hearts from unirradiated rats (Fig. 6). In 6/10 irradiated rats, we observed rare foci of chronic (lymphocytic) inflammation in the myocardium (Fig. 6B and E), usually constituting 10–20 lymphocytes surrounding a myocyte or blood vessel. These foci of inflammation were not reproducibly localized to a single ventricle or an area of the ventricular wall. In one animal, this inflammation was associated with a single focus of myocyte damage (Fig. 6C and F). The heart of one irradiated animal contained hemosiderin-laden macrophages surrounding small blood vessels in the myocardium (consistent with prior injury), but no other inflammation. Outside of these foci, there was no evidence of myocardial or vascular injury or fibrosis.

Analysis of pleural effusions (see Table 3)

Gross pleural effusions were recorded in 60% of rats (n = 6/10) that met IACUC criteria for euthanasia between 5 and 8 weeks after 15 Gy. In studies terminated at 6 weeks, 76% of rats (from n = 33) had pleural effusions. Lung weights in rats without pleural effusions were higher than those of rats with effusions (1.8 ± 0.2 g, n = 6 vs 1.4 ± 0.3 g, n = 9;

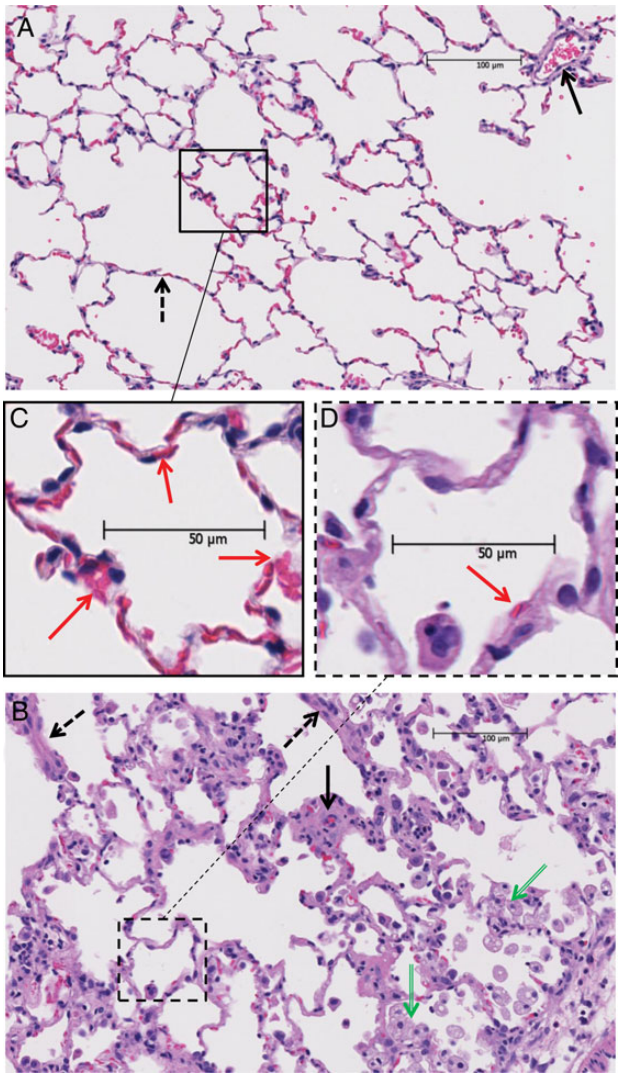

Fig. 4. Radiation-induced changes in representative H&E-stained lung sections (4 µm thick) pointing out four categories scored in Table 1: (**A**) lung from unirradiated rat; (**B**) lung from irradiated (15 Gy) rat; (**C**) magnified image of boxed area in A. (**D**) magnified image of boxed area in B. Solid and dashed arrows in (A) point to blood vessels and alveolar walls respectively, which appear thicker in the irradiated lung (B). Green arrows in the irradiated lung section (B) point to abundant foamy macrophages. Red arrows point to red blood cells. Note the well perfused alveolar capillaries in unirradiated lungs (C) as compared with the poorly perfused capillaries in irradiated lungs (D).

$P = 0.008$). Values for parameters used to define transudative versus exudative effusions in humans by Light's and related criteria are shown in Table 3A. Table 3B describes the total and differential cell count from seven randomly selected effusions, indicating the presence of mostly inflammatory cells such as macrophages. Mast cells were present in the majority of samples. Based on these results, most effusions were described as modified transudates to reflect shared characteristics of both transudation and exudation.

DISCUSSION

To study the pathophysiological sequences leading to death after thoracic irradiation in the rat we administered 15 Gy to the whole thorax, which was previously shown to cause 100% lethality from pneumonitis [2]. Our goal was to examine the role of the heart and radiation-associated pleural effusions in this morbidity. This model provides several new insights. First, we are unaware of other studies that have quantified oxygenation status in rats after thoracic radiation. Second, concurrent with profound hypoxia, we observed severe pulmonary hypertension with right ventricular enlargement and echocardiographic signs of pressure and volume overload, and associated left ventricular dysfunction such that cardiac output was decreased to ~30% of that in control rats. In the context of increased pulmonary vascular resistance, which we have previously reported for whole-thorax irradiation [9, 39], these data suggest the occurrence of hypoxic pulmonary pathophysiology with secondary cardiac remodeling and decreased cardiac output [40] following a radiation dose to the thorax that is considered subthreshold for direct cardiac damage (Fig. 7). Minimal to no histological cardiac pathology was observed in our rats following irradiation, and the rare foci of mild lymphocytic inflammation would not account for the cardiac dysfunction or explain the pleural effusions observed in irradiated rats. Third, although pleural effusions are a well-recognized consequence of thoracic radiation in rodents, our study indicated that these effusions can be quantified and characterized biochemically and cytologically. We conclude that radiation-induced pleural effusions in the rats appear to be attributable to both hydrostatic (low left ventricular output) and inflammatory mechanisms; they are associated with a cellular component that includes a variety of leukocytes, and have biochemical values consistent with both exudative and transudative processes. The extent to which our findings extend to male (or elderly) rodents or to other strains remains to be determined.

Our long-term goal is to develop mitigators for radiation injuries to the lung induced by a single dose of ionizing radiation at doses relevant to a radiological attack or nuclear accident. The National Institutes of Health (USA) has initiated a radiation countermeasures development program that requires such mitigators to be approved under the Federal Drug Administration (USA) 'animal rule', since relevant high single-doses of radiation cannot be ethically delivered to humans [41]. For this reason, animal models that reproduce radiation injuries in humans are required. Rodents are the animal models of choice, because they are well characterized, easy to work with, and have genetically altered strains available for advanced research [41, 42]. Thus the pathophysiology of radiation injury needs to be determined in animal models to successfully navigate the FDA animal rule.

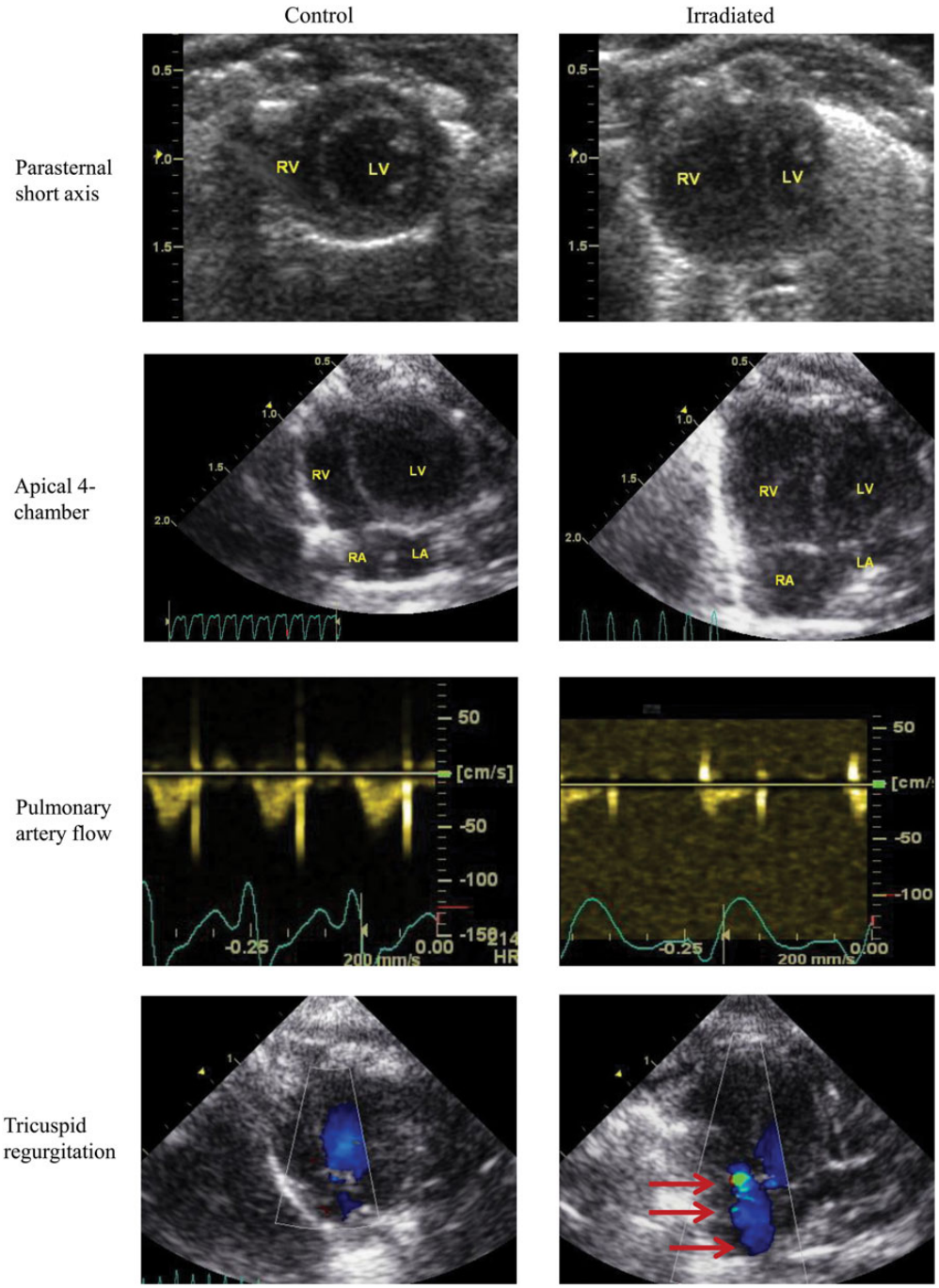

Fig. 5. Echocardiographic evidence of pulmonary artery hypertension in irradiated rats**.** Columns represent control rats (left-side) or irradiated rats (right-side) and rows represents four different imaging windows: (1) parasternal short-axis, (2) apical four-chamber views using B-mode at end-diastole to demonstrate right ventricular remodeling, (3) high parasternal short-axis view with pulsed-wave Doppler is used to detect pulmonary artery flow, and (4) apical four-chamber view with color Doppler is used to detect tricuspid regurgitation (red arrows). The parasternal short axis and apical four-chamber views show right ventricular dilatation with concomitant decrease in left ventricle. The pulmonary artery profiles reflect the presence of pulmonary hypertension. Normal, round-shaped flow profile is found in the control hearts, whereas a blunted flow profile with a sharp peak at early systole and a decreased acceleration time and increased deceleration is seen in the irradiated rat heart. There is no detectable tricuspid regurgitation by color Doppler in control rats, but tricuspid regurgitation is common in the irradiated group. R = right, L = left, A = atrium, V = ventricle.

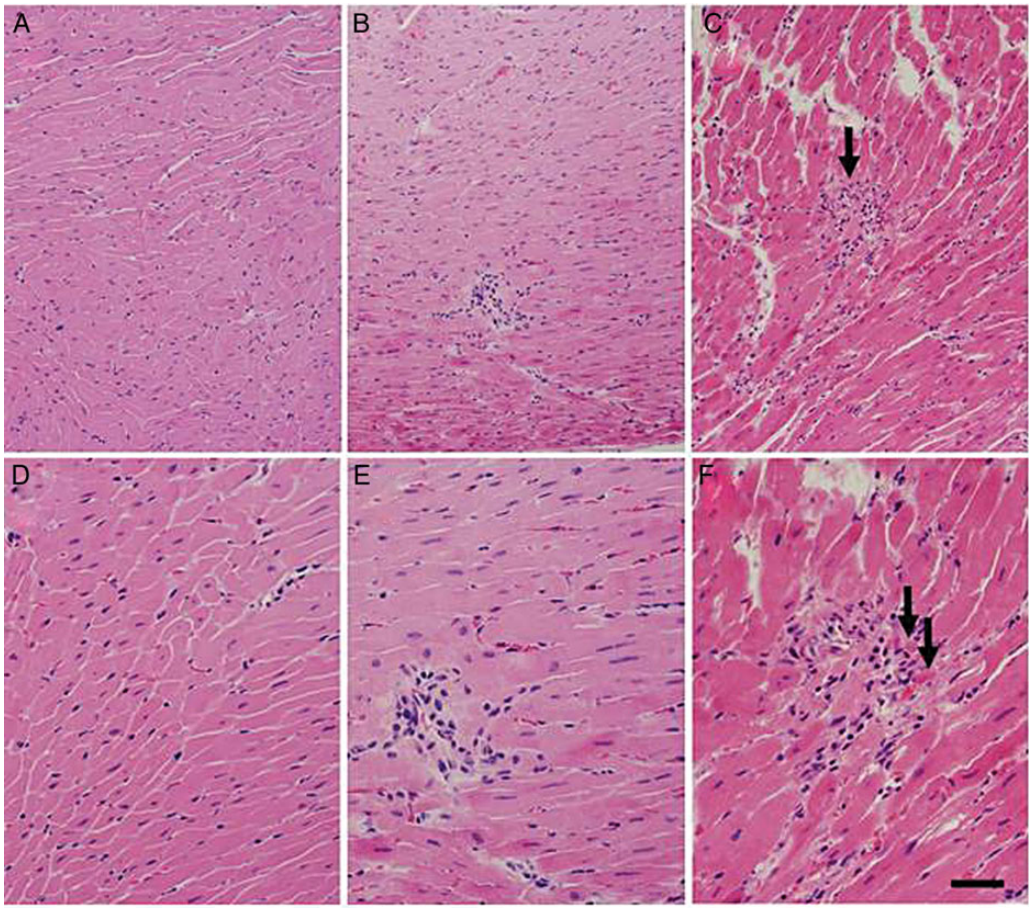

Fig. 6. Histological findings in irradiated rat hearts. H&E stains of hearts taken at two magnifications from unirradiated (**A** and **D**) and irradiated (**B**, **C**, **E** and **F**) rats reveal scattered foci of lymphocytic inflammation in a subpopulation of irradiated rats. One irradiated rat showed cardiac myocyte necrosis (C and F, arrows) associated with lymphocytic inflammation. Bars = 80 μm (A, B and C) and 40 μm (D, E and F).

Our previous studies, and those of others [3, 6, 9], indicate that injury to the pulmonary vascular endothelium and vessel wall reduce vascular reactivity after 10 Gy to the thorax [10]. Blood vessels are also less distensible than in unirradiated rats [9], and increased pulmonary vascular resistance was measured in lungs *ex vivo*. Vascular dropout was seen by angiography [9]. Vascular injury and dropout along with inflammatory infiltrates could hinder the ability of the lung to match perfusion with ventilation, consistent with hypoxemia. We have observed compensatory RVH after a non-lethal dose of irradiation (10 Gy) [9]. Higher doses of irradiation in a different strain of Wistar rats induced perivascular and pulmonary edema with increased pulmonary artery pressure and left ventricular relaxation times, indicative of biventricular diastolic dysfunction [6, 7]. The authors of the latter study concluded that irradiation of the heart and lung enhanced the severity of radiation pneumonitis [6, 7] although description of pleural effusions was minimal as compared to earlier studies in rats [20, 21]. Interactions between the irradiated heart and lungs have also been reported after localized irradiation of the heart [6, 8]. In the present study, we observed hypoxia, pulmonary hypertension, reduction in left ventricular diameter at diastole and decreased cardiac output at 6 weeks following a lethal whole-thorax dose. These data do not exclude direct effects of radiation on the heart, but provide sufficient pathophysiology to explain morbidity based primarily on pulmonary responses to radiation (Figs 3 and 7).

The pathophysiological link between cardiac remodeling and radiation-induced changes to the lung is strengthened by three observations. First, with lower doses of thoracic radiation (10 Gy) that allow rats to survive pneumonitis, spontaneous recovery from lung pathology is associated with reversal of RVH [9]. With lower radiation doses that produced limited pneumonitis (5 Gy), no RVH was identified at times corresponding to pneumonitis. Second, thoracic radiation inducing pneumonitis is accompanied by pulmonary vascular dropout, decreased pulmonary vascular distensibility and increased vascular resistance, changes that induce right heart remodeling. Third, mitigation of lung injury after

Table 3: Summary of pleural effusion in irradiated (15 Gy) rats after 42 days

A. Pleural fluid	**# Transudate**	**# Exudate**
Appearance		
Criteria	**Clear**	**Cloudy**
15 Gy rats	0/9	9/9 (mean 2.4 ± 0.7)
Specific gravity		
Criteria	**≤1.012**	**≥1.020**
15 Gy rats	0/9	9/9 (mean 1.023 ± 0.003)
Fluid:serum protein		
Light's criteria	**<0.5**	**>0.5**
15 Gy rats	1/7 (0.19)	6/7 (mean 0.73 ± 0.2)
Fluid:serum LDH		
Light's criteria	**<0.6**	**>0.6**
15 Gy rats	7/7 (mean 0.4 ± 0.1)	0/7
Cholesterol (mg/dl)		
Criteria	**<45**	**>45**
15 Gy rats	8/9 (mean 32 ± 8)	1/9 (48)

B. Differential cell count for individual rats

# white blood cells (wbc)/µl	**% Macrophages/large monocytes**	**% monocytes**	**% lymphocytes**	**% neutrophils**	**% mast cells**
1060	35	–	59	4	–
2870	87	–	4	6	3
1530	85	–	6	7	2
176	80	–	3	8	1
2900	87	–	3	3	7
492	93	–	–	1	rare
290	95	3	–	2	–

A = criteria for classifying human effusions (values for human effusions are included in bold font). B = differential cell count.

thoracic radiation by angiotensin-converting enzyme (ACE) inhibitors yields decreased pneumonitis, decreased pulmonary vascular dropout, increased pulmonary vascular distensibility, decreased pulmonary vascular resistance and improved survival [2, 39, 43]. The pathophysiological consequences of radiation-induced pleural effusion remain to be fully resolved. Effusions were not reported as present or absent in early studies of whole-lung irradiation in humans [13–16]. Clinically, patients with heart failure can develop pleural effusions resulting from increased interstitial fluid in the lung caused by elevated hydrostatic pressure [40]. Typically this occurs in patients with left-sided heart failure, but it has also been seen occasionally in patients with right-sided heart failure. Fluid moves from the pulmonary interstitial space across the visceral pleura into the pleural space along a pressure gradient. In this case, the fluid is typically a transudate, though 25% of cases may fall into the exudative category. Radiation injury to the lymphatics may also be a contributing factor to impaired drainage of the pleural space [18].

In rodents, congestive heart failure is reported to lead to a 'protein rich transudate' [44]. Effusions are caused primarily by increased alveolar capillary pressures, and decreased cardiac output [44], the latter of which we observed. Venous congestion leads to increased pressure in the posterior vena cava, reducing lymphatic drainage from the pleural cavity. Such transudates have a relatively high protein content because the vessels become permeable to plasma proteins [44]. Exudates form when there is increased vascular permeability caused by inflammatory cells accompanied by migration of (mostly) neutrophils [44]. Frequently a mixture of macrophages and lymphocytes accompany the neutrophils. High-volume pleural effusions (up to 10 ml) have been noted

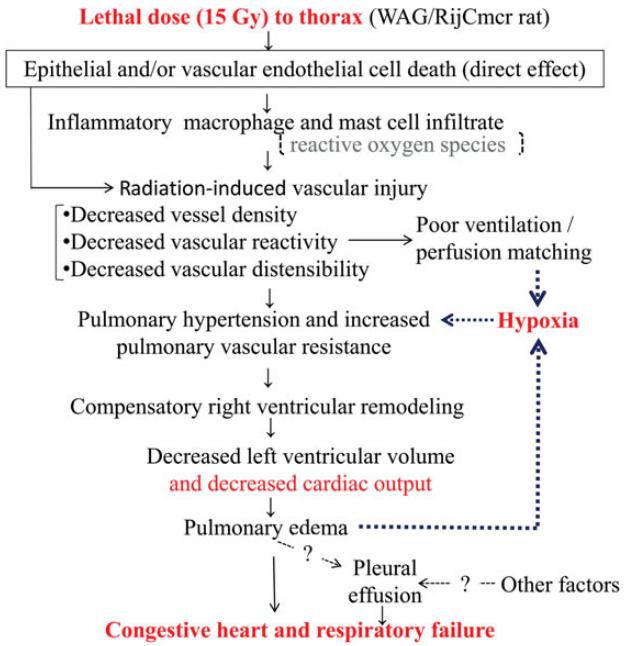

Fig. 7. Schematic of possible events leading to lethal radiation pneumonitis.

in Wistar rats following whole-thorax irradiation [20, 21]. Because thoracic volumes are constrained by boney structures, large pleural effusions restrict lung parenchymal volume. When interstitial or alveolar fluid moves into the pleural space, it is reasonable to expect that lungs of rats with pleural effusion would weigh less than those with pulmonary edema but no pleural effusion, as we observed.

In the current study, pleural effusions were classified as modified transudates by a CLIA-approved veterinary laboratory. The samples qualified as exudates based on the criteria for human effusions (e.g. protein content and cholesterol ratios), but were transudative based on lactate dehydrogenase (LDH). In addition, the predominant cellular constituents were macrophages and large monocytes, as compared with neutrophils. One of the most striking characteristics of effusions in this study is the presence of mast cells (Table 3B). These cells are increased in irradiated rat lungs [5, 45]. Mast and other infiltrating cells release inflammatory mediators and cytokines in irradiated lungs that can alter vascular permeability and promote pulmonary hypertension. Thus, we postulate that pleural effusions occurring in rats after lethal doses of radiation may be due to a combination of multiple factors. These would include hypoxia-induced increase in pulmonary vascular resistance, right ventricular remodeling and impaired left ventricular function with transudative effusions, conditions that would result in congestive heart failure. Also, an increase in vascular permeability via inflammatory mediators secreted by infiltrating immune cells in irradiated lungs would promote exudative types of effusion. Radiation injury to the draining lymphatic system could also lead to exudative pleural effusions.

Pleural effusions are common in mice after whole-thorax irradiation, but not always coincidental with pneumonitis [19]; the status of the hearts in these mice has not been reported [11, 19]. Effusions in CBA mice arise independently after the resolution of pneumonitis, and fall in an exudative category [19]. Interestingly, some mouse strains, (e.g. BALB/c) show early pleural effusions with pneumonitis, as observed in our rats. This mouse strain also exhibits a strong mast cell infiltration in the lung, but the connection to pulmonary hypertension and cardiac injury remains to be explored [45]. Effusions were observed after whole-thoracic irradiation of non-human primates, with a frequency as high as 75% at 12 Gy [46]. It was common to encounter radiation-associated pleural effusions in humans undergoing radiotherapy [1]; but improvements in dose-delivery and treatment planning have largely prevented lethal pneumonitis, and so pleural effusions may now be less frequent in this population. Dexamethasone eliminated lethal pleural fluid accumulation in rats (and possibly in primates) after partial-body irradiation [46, 47]; thus the standard clinical use of steroids and diuretics to treat radiation pneumonitis and effusions may also account for the low reported incidence of pleural effusions in patients receiving radiotherapy.

One of the first, and most successful to date, class of countermeasures described for lung injury, ACE inhibitors, also reduce blood pressure and improve pathological vascular remodeling [48]. Since we present evidence that vascular injury and pulmonary artery hypertension play a role in radiation pneumonitis, ACE inhibitors may be expected to mitigate lung injury as well as improve survival after radiation. In fact, these drugs have improved pulmonary-related outcomes after radiotherapy in the clinic [49, 50]. In summary, a better understanding of the sequence of pathophysiological events of radiation pneumonitis will enable therapeutic intervention after radiological events or radiotherapy.

ACKNOWLEDGEMENTS

We thank Marylou Mader for excellent animal care and technical assistance and Dr Eric P. Cohen for his helpful comments. Histological preparation and staining was performed by the Pediatric BioBank and the Analytical Tissue Core at the Medical College of Wisconsin, with support from the MACC Fund.

CONFLICT OF INTEREST

The authors report that there are no conflicts of interest concerning the materials or methods used in this study or the findings specified in this paper.

FUNDING

This work was supported by the National Institutes of Health / National Institute of Allergy and Infectious Diseases (NIAID) AI81294, AI101898 and AI107305 to M.M.; AI067734 to J.E.M and National Heart Lung and Blood Institute (NHLBI) HL116530 to E.R.J. and the Veterans Administration Merit Review (BX001681 to E.R.J.). Funding to pay the Open Access publication charges for this article was provided by AI101898 and AI107305.

REFERENCES

1. Gross NJ. Pulmonary effects of radiation therapy. *Ann Intern Med* 1977;**86**:81–92.
2. Medhora M, Gao F, Fish BL *et al*. Dose-modifying factor for captopril for mitigation of radiation injury to normal lung. *J Radiat Res* 2012;**53**:633–40.
3. Travis EL, Harley RA, Fenn JO *et al*. Pathologic changes in the lung following single and multi-fraction irradiation. *Int J Radiat Oncol Biol Phys* 1977;**2**:475–90.
4. Vergara JA, Raymond U, Thet LA. Changes in lung morphology and cell number in radiation pneumonitis and fibrosis: a quantitative ultrastructural study. *Int J Radiat Oncol Biol Phys* 1987;**13**:723–32.
5. Szabo S, Ghosh SN, Fish BL *et al*. Cellular inflammatory infiltrate in pneumonitis induced by a single moderate dose of thoracic X radiation in rats. *Radiat Res* 2010; **173**:545–56.
6. Ghobadi G, Bartelds B, van der Veen SJ *et al*. Lung irradiation induces pulmonary vascular remodelling resembling pulmonary arterial hypertension. *Thorax* 2012;**67**:334–41.
7. Ghobadi G, van der Veen S, Bartelds B *et al*. Physiological interaction of heart and lung in thoracic irradiation. *Int J Radiat Oncol Biol Phys* 2012;**84**:e639–46.
8. Geist BJ, Lauk S, Bornhausen M *et al*. Physiologic consequences of local heart irradiation in rats. *Int J Radiat Oncol Biol Phys* 1990;**18**:1107–13.
9. Ghosh SN, Wu Q, Mader M *et al*. Vascular injury after whole thoracic x-ray irradiation in the rat. *Int J Radiat Oncol Biol Phys* 2009;**74**:192–9.
10. Zhang R, Ghosh SN, Zhu D *et al*. Structural and functional alterations in the rat lung following whole thoracic irradiation with moderate doses: injury and recovery. *Int J Radiat Biol* 2008;**84**:487–97.
11. Jackson IL, Vujaskovic Z, Down JD. Revisiting strain-related differences in radiation sensitivity of the mouse lung: recognizing and avoiding the confounding effects of pleural effusions. *Radiat Res* 2010;**173**:10–20.
12. Fryer CJ, Fitzpatrick PJ, Rider WD *et al*. Radiation pneumonitis: experience following a large single dose of radiation. *Int J Radiat Oncol Biol Phys* 1978;**4**:931–6.
13. Keane TJ, Van Dyk J, Rider WD. Idiopathic interstitial pneumonia following bone marrow transplantation: the relationship with total body irradiation. *Int J Radiat Oncol Biol Phys* 1981;**7**:1365–70.
14. Van Dyk J, Keane TJ, Kan S *et al*. Radiation pneumonitis following large single dose irradiation: A re-evaluation based on absolute dose to lung. *Int J Radiat Oncol Biol Phys* 1981;**7**:461–67.
15. Sampath S, Schultheiss TE, Wong J. Dose response and factors related to interstitial pneumonitis after bone marrow transplant. *Int J Radiat Oncol Biol Phys* 2005; **63**:876–84.
16. Bate D, Gutterman RJ. Changes in lung and pleura following two-million-volt therapy for carcinoma of the breast. *Radiology* 1957;**69**:372–83.
17. Bachman AL, Macken K. Pleural effusions following supervoltage radiation for breast carcinoma. *Radiology* 1959;**72**:699–709.
18. Morrone N, Gama e Silva Volpe VL, Dourado AM *et al*. Bilateral pleural effusion due to mediastinal fibrosis induced by radiotherapy. *Chest* 1993;**104**:1276–78.
19. Jackson IL, Vujaskovic Z, Down JD. A further comparison of pathologies after thoracic irradiation among different mouse strains: finding the best preclinical model for evaluating therapies directed against radiation-induced lung damage. *Radiat Res* 2011;**175**:510–18.
20. Down JD. The nature and relevance of late lung pathology following localised irradiation of the thorax in mice and rats. *Br J Cancer Suppl* 1986;**7**:330–32.
21. van Rongen E, Tan CH, Durham SK. Late functional, biochemical and histological changes in the rat lung after fractionated irradiation to the whole thorax. *Radiother Oncol* 1987;**10**:231–46.
22. Sarkisova K, van Luijtelaar G. The WAG/Rij strain: a genetic animal model of absence epilepsy with comorbidity of depression [corrected]. *Prog Neuropsychopharmacol Biol Psychiatry* 2011;**35**:854–76.
23. Gao F, Fish BL, Moulder JE *et al*. Enalapril mitigates radiation-induced pneumonitis and pulmonary fibrosis if started 35 days after whole-thorax irradiation. *Radiat Res* 2013;**180**:546–52.
24. Cohen EP, Molteni A, Hill P *et al*. Captopril preserves function and ultrastructure in experimental radiation nephropathy. *Lab Invest* 1996;**75**:349–60.
25. Rockwell S, Kelley M, Rosiello RA *et al*. Administration of a perfluorochemical emulsion plus carbogen breathing does not alter radiation pneumonitis. *Proc Soc Exp Biol Med* 1995;**208**: 288–93.
26. Rosiello RA, Merrill WW, Rockwell S *et al*. Radiation pneumonitis. Bronchoalveolar lavage assessment and modulation by a recombinant cytokine. *Am Rev Respir Dis* 1993;**148**: 1671–6.
27. van Rongen E, Tan C, Zurcher C. Early and late effects of fractionated irradiation of the thorax of WAG/Rij rats. *Br J Cancer* 1986;**53**:333–5.
28. van Rongen E, Madhuizen HT, Tan CH *et al*. Early and late effects of fractionated irradiation and the kinetics of repair in rat lung. *Radiother Oncol* 1990;**17**:323–37.
29. Landuyt W, Fowler J, Ruifrok A *et al*. Kinetics of repair in the spinal cord of the rat. *Radiother Oncol* 1997;**45**: 55–62.
30. Moulder JE, Cohen EP, Fish BL *et al*. Prophylaxis of bone marrow transplant nephropathy with captopril, an inhibitor of angiotensin-converting enzyme. *Radiat Res* 1993;**136**:404–7.

31. Doctrow SR, Lopez AM, Schock A *et al*. A synthetic superoxide dismutase/catalase mimetic EUK-207 mitigates radiation dermatitis and promotes wound healing in irradiated skin. *J Investig Dermatol* 2013;**133**:1088–96.
32. Gao F, Narayanan J, Joneikis C *et al*. Enalapril mitigates focal alveolar lesions, a histological marker of late pulmonary injury by radiation to the lung. *Radiat Res* 2013;**179**:465–74.
33. Baker JE, Fish BL, Su J *et al*. 10 Gy total body irradiation increases risk of coronary sclerosis, degeneration of heart structure and function in a rat model. *Int J Radiat Biol* 2009;**85**:1089–100.
34. Lenarczyk M, Lam V, Jensen E *et al*. Cardiac injury following 10 Gy total body irradiation: indirect role of effects on abdominal organs. *Radiat Res* 2013;**180**:247–58.
35. Hopewell JW, Rezvani M, Moustafa HF. The pig as a model for the study of radiation effects on the lung. *Int J Radiat Biol* 2000;**76**:447–52.
36. Gao F, Fish BL, Szabo A *et al*. Short-term treatment with a SOD/catalase mimetic, EUK-207, mitigates pneumonitis and fibrosis after single-dose total-body or whole-thoracic irradiation. *Radiat Res* 2012;**178**:468–80.
37. Bernard SL, An D, Glenny RW. Validation of the Nonin 8600V Pulse Oximeter for heart rate and oxygen saturation measurements in rats. *Contemp Top Lab Anim Sci* 2004;**43**:43–45.
38. Sonin DL, Wakatsuki T, Routhu KV *et al*. Protease-activated receptor 1 inhibition by SCH79797 attenuates left ventricular remodeling and profibrotic activities of cardiac fibroblasts. *J Cardiovasc Pharmacol Ther* 2013;**18**:460–75.
39. Molthen RC, Wu Q, Fish BL *et al*. Mitigation of radiation induced pulmonary vascular injury by delayed treatment with captopril. *Respirology* 2012;**17**:1261–68.
40. Porcel JM. Pleural effusions from congestive heart failure. *Semin Respir Crit Care Med* 2010;**31**:689–97.
41. DiCarlo AL, Jackson IL, Shah JR *et al*. Development and licensure of medical countermeasures to treat lung damage resulting from a radiological or nuclear incident. *Radiat Res* 2012;**177**:717–21.
42. Williams JP, Brown SL, Georges GE *et al*. Animal models for medical countermeasures to radiation exposure. *Radiat Res* 2010;**173**:557–78.
43. Ghosh SN, Zhang R, Fish BL *et al*. Renin–angiotensin system suppression mitigates experimental radiation pneumonitis. *Int J Radiat Oncol Biol Phys* 2009;**75**:1528–36.
44. Stockham S, Scott M. Cavitary effusions. In: Stockham S, Scott M (eds). *Fundamentals of Veterinary Clinical Pathology*, 2nd edn. Ames, IA: Blackwell Publishing, 2008, 831–68.
45. Down JD, Medhora M, Jackson IL *et al*. Do variations in mast cell hyperplasia account for differences in radiation-induced lung injury among different mouse strains, rats and nonhuman primates? *Radiat Res* 2013;**180**:216–21.
46. Garofalo M, Bennett A, Farese AM *et al*. The delayed pulmonary syndrome following acute high-dose irradiation: a rhesus macaque model. *Health Phys* 2014;**106**:56–72.
47. Geraci JP, Mariano MS, Jackson KL *et al*. Effects of dexamethasone on late radiation injury following partial-body and local organ exposures. *Radiat Res* 1992;**129**:61–70.
48. Lang CC, Struthers AD. Targeting the renin–angiotensin–aldosterone system in heart failure. *Nat Rev Cardiol* 2013;**10**: 125–34.
49. Kharofa J, Cohen EP, Tomic R *et al*. Decreased risk of radiation pneumonitis with incidental concurrent use of angiotensin-converting enzyme inhibitors and thoracic radiation therapy. *Int J Radiat Oncol Biol Phys* 2012;**84**:238–43.
50. Cohen EP, Bedi M, Irving AA *et al*. Mitigation of late renal and pulmonary injury after hematopoietic stem cell transplantation. *Int J Radiat Oncol Biol Phys* 2012;**83**:292–96.